ACS ORGANIC & INORGANIC Au
AN OPEN ACCESS JOURNAL OF THE AMERICAN CHEMICAL SOCIETY

pubs.acs.org/orginorgau

Article

The Question of the Redox Site in Metal−Metal Multiple-Bonded Metallocorrole Dimers

W. Ryan Osterloh, Jeanet Conradie, Abraham B. Alemayehu, Abhik Ghosh,* and Karl M. Kadish*

Cite This: *ACS Org. Inorg. Au* 2023, 3, 35−40

Read Online

ACCESS | Metrics & More | Article Recommendations | Supporting Information

ABSTRACT: We have revisited the electrochemistry of metallocorrole dimers with low-temperature cyclic voltammetry and UV−visible−NIR spectroelectrochemistry, with the aim of determining the sites of the redox processes undergone by these compounds. The systems studied include the metal−metal triple-bonded complexes $\{Ru[TpOMePC]\}_2$ and $\{Os[TpOMePC]\}_2$ and the metal−metal quadruple-bonded complex $\{Re[TPC]\}_2$, where T*p*OMePC and TPC refer to trianionic *meso*-tris(*p*-methoxyphenyl)corrole and *meso*-triphenylcorrole ligands. For all three compounds, the first oxidation potentials are found at 0.52 ± 0.04 V vs SCE in CH_2Cl_2/0.1 M TBAP and are accompanied by major changes in the optical spectra, especially the appearance of broad, low-energy bands, suggesting macrocycle-centered oxidation in each case. In contrast, the reduction potentials span an 800 mV range, occurring at $E_{1/2}$ = −0.52 V for $\{Re[TPC]\}_2$, −0.81 V for $\{Ru[TpOMePC]\}_2$, and −1.32 V for $\{Os[TpOMePC]\}_2$, with more modest changes in the optical spectra, implying a significant metal-centered character in the reduction process. Density functional theory (DFT) calculations largely (but not entirely) bear out these expectations. The combined experimental and theoretical data indicate that one-electron addition to the Re dimer involves the Re−Re δ^* LUMO, while one-electron addition to the Ru dimer largely involves the Ru−Ru π^* LUMO. In contrast, the calculations suggest that one-electron reduction of the Os dimer occurs largely on the corrole ligands, a phenomenon attributed to the relativistic destabilization of the Os−Os π^* MOs.

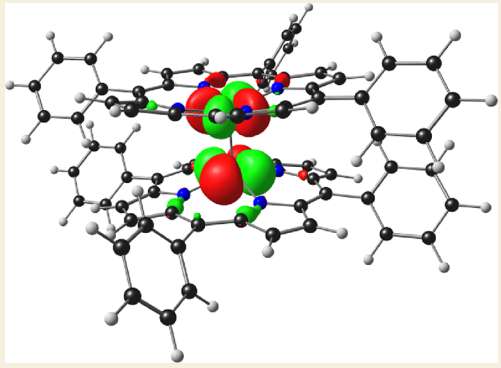

KEYWORDS: *quadruple bond, metal−metal bond, spectroelectrochemistry, density functional theory, relativistic effect*

INTRODUCTION

Almost 60 years ago, Cotton recognized the possibility of metal−metal quadruple bonding in the $Re_2Cl_8^{2-}$ dianion.[1,2] Since then, the field of metal−metal bonding has grown enormously and has been the subject of numerous review articles.[3−8] Nevertheless, significant gaps remain in our knowledge about quadruple bonds, notably in relation to their electrochemical behavior. As far as we are able to discern, the recent synthesis of rhenium corrole dimers in one of our laboratories allowed the first determination of the reduction potential of a quadruple-bonded system.[9] Surprisingly enough, analogous measurements on quadruple-bonded Mo and W porphyrin dimers have not been reported.[10−13] Such measurements are also lacking for quadruple-bonded systems with nonporphyrin supporting ligands.[14−16] Indeed, in general, UV−visible−NIR spectroelectrochemical studies on metal−metal multiple-bonded systems are conspicuous by their absence. Except for a handful of studies on triple-bonded Ru corrole dimers,[17−19] there is little experimental information on the site of oxidation and reduction of multiple-bonded metalloporphyrin and metallocorrole dimers.

To address this question, we have revisited the electrochemistry of three metallocorrole dimers, with cyclic voltammetry (at room and low-temperature) and thin-layer UV−vis−NIR spectroelectrochemistry experiments. The systems studied include the metal−metal triple-bonded complexes $\{Ru[TpOMePC]\}_2$[20] and $\{Os[TpOMePC]\}_2$[21] and the metal−metal quadruple-bonded complex $\{Re[TPC]\}_2$,[9] where T*p*OMePC and TPC refer to the trianionic *meso*-tris(*p*-methoxyphenyl)corrole and *meso*-triphenylcorrole ligands. In conjunction with with scalar-relativistic density functional theory (DFT) calculations, the results provide a first comparative account of metal- versus ligand-centered redox processes across the main classes of multiple-bonded metallocorrole dimers synthesized to date.

RESULTS AND DISCUSSION

Figures 1 and 2 present cyclic voltammograms (CVs) of the three complexes, studied at room temperature and at −60 °C,

Received: June 16, 2022
Revised: October 6, 2022
Accepted: October 7, 2022
Published: October 26, 2022

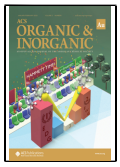

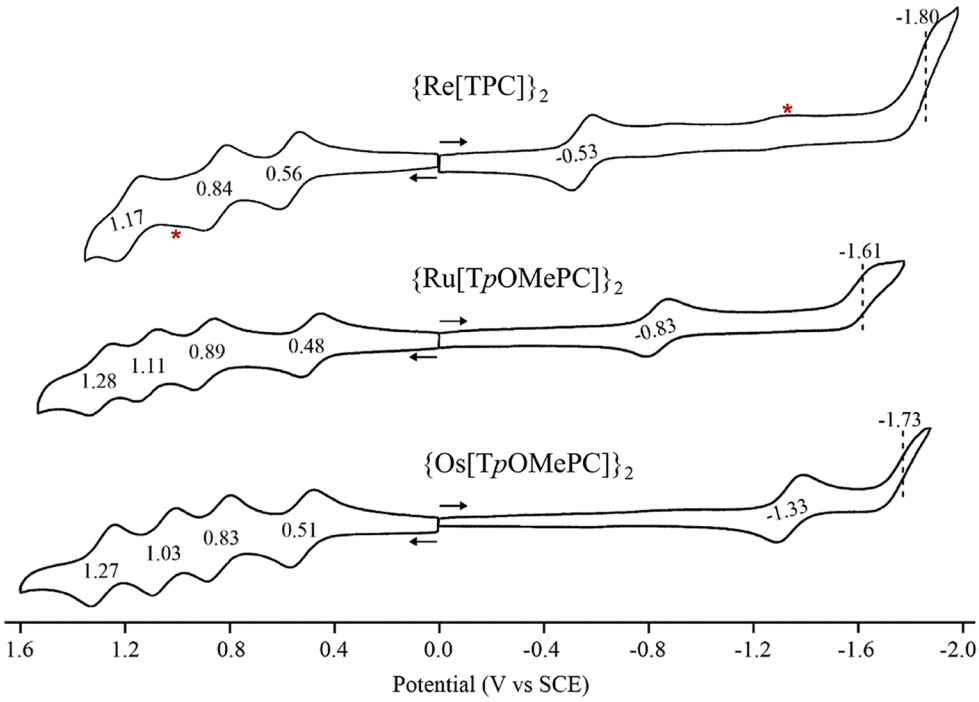

Figure 1. Cyclic voltammograms of the metal−metal bonded corrole dimers in CH_2Cl_2 containing 0.1 M TBAP at room temperature. Scan rate = 0.1 V/s. Currents marked with an asterisk are tentatively assigned to trace rhenium-oxo species in solution or at the electrode surface.

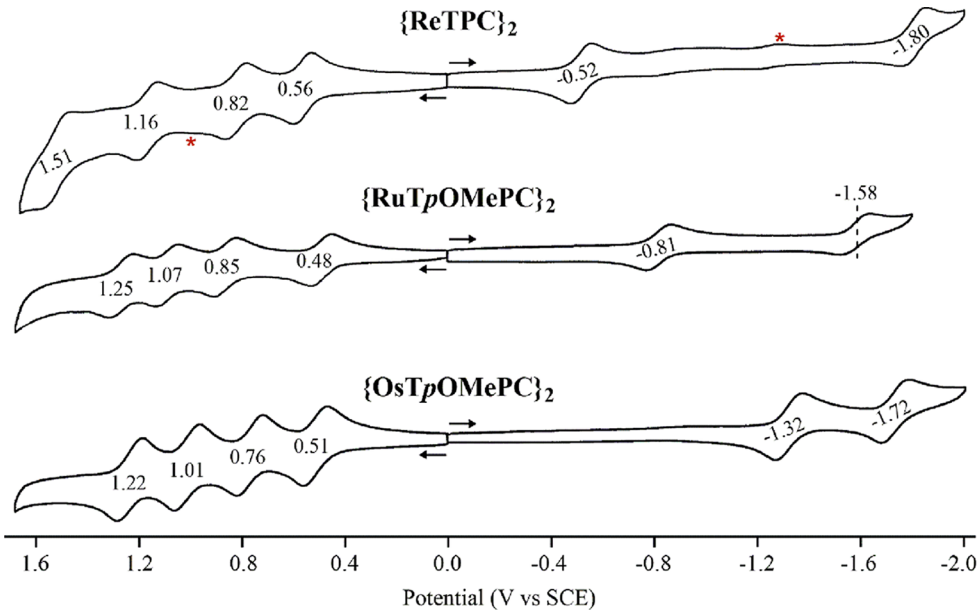

Figure 2. Cyclic voltammograms of the metal−metal bonded corrole dimers in CH_2Cl_2 containing 0.1 M TBAP at −60 °C. Scan rate = 0.1 V/s. Currents marked with an asterisk are tentatively assigned to trace rhenium-oxo species in solution or at the electrode surface.

Table 1. Redox Potentials (V vs. SCE) of {Re[TPC]}$_2$, {Ru[T*p*OMePC]}$_2$, and {Os[T*p*OMePC]}$_2$ in CH_2Cl_2 Containing 0.1 M TBAP at −60 °C.

complex	$E_{1/2ox4}$	$E_{1/2ox3}$	$E_{1/2ox2}$	$E_{1/2ox1}$	$E_{1/2red1}$	$E_{1/2red2}$	ΔE
{Re[TPC]}$_2$	1.51	1.16	0.82	0.56	−0.52	−1.80	1.08
{Ru[T*p*OMePC]}$_2$	1.25	1.07	0.85	0.48	−0.81	−1.58	1.39
{Os[T*p*OMePC]}$_2$	1.22	1.01	0.76	0.51	−1.32	−1.72	1.83

respectively. In general (with one exception), the CVs exhibit four reversible oxidations and two reversible reductions, although the reversibility of the second reduction is distinctly clearer at the lower temperature. A striking observation is that while the oxidation potentials (with the exception of $E_{1/2ox4}$) are nearly identical across the four compounds (and largely

https://doi.org/10.1021/acsorginorgau.2c00030
ACS Org. Inorg. Au 2023, 3, 35−40

comparable to those observed with metallocorroles with redox-inactive metal centers[20,22−37]), the reduction potentials vary dramatically (Table 1). These findings may be naively interpreted as suggesting corrole-centered oxidations and metal-centered reductions in each case. Some support for this finding is already present in the literature from preliminary DFT calculations.[9,21]

Figures 3−5 present spectral changes associated with controlled-potential reduction of the compounds studied,

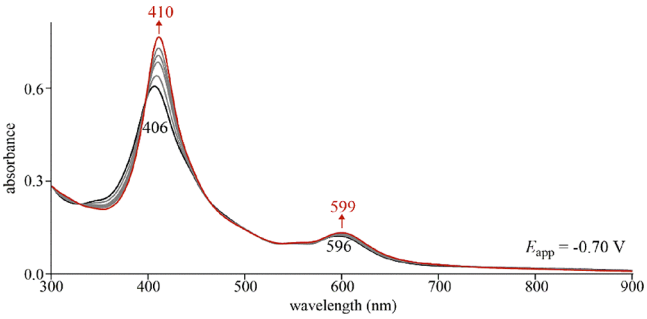

Figure 3. Fully reversible UV−vis spectral changes of $\{Re[TPC]\}_2$ during the first reduction in CH_2Cl_2/0.1 M TBAP.

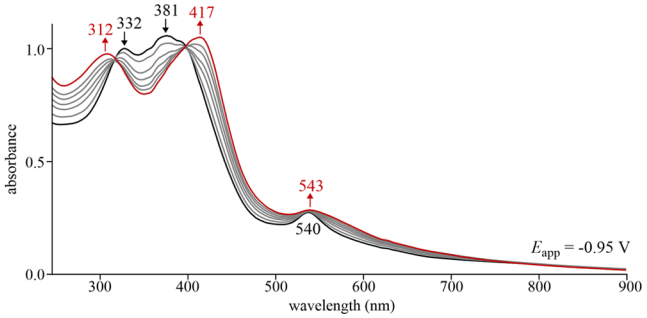

Figure 4. Fully reversible UV−vis spectral changes of $\{Ru[TpOMePC]\}_2$ during the first reduction in CH_2Cl_2/0.1 M TBAP.

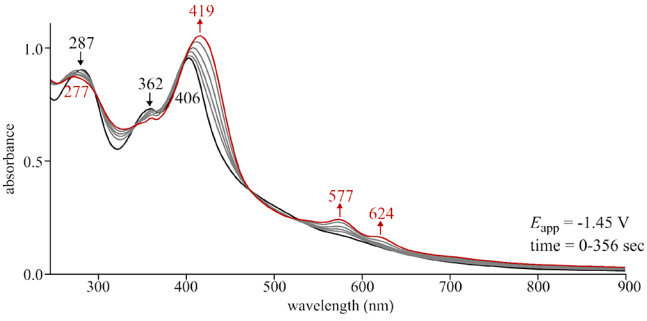

Figure 5. UV−vis spectral changes of $\{OsTpOMePC\}_2$ during the first reduction in CH_2Cl_2/0.1 M TBAP. *Note*: This process was found to be irreversible on the thin layer time scale.

while Figures 6−8 present similar results for controlled-potential oxidation. It is clear that reduction does not result in major spectral changes; even for the Ru complex, for which the changes are most significant, there is little change in the intensity of the Soret bands. In contrast, oxidation results (Figures 6−8) in major spectral changes, especially the appearance of a broad band between 673 and 700 nm that is indicative of a corrole radical. Overall, the results suggest that electron addition does not significantly affect the aromaticity of

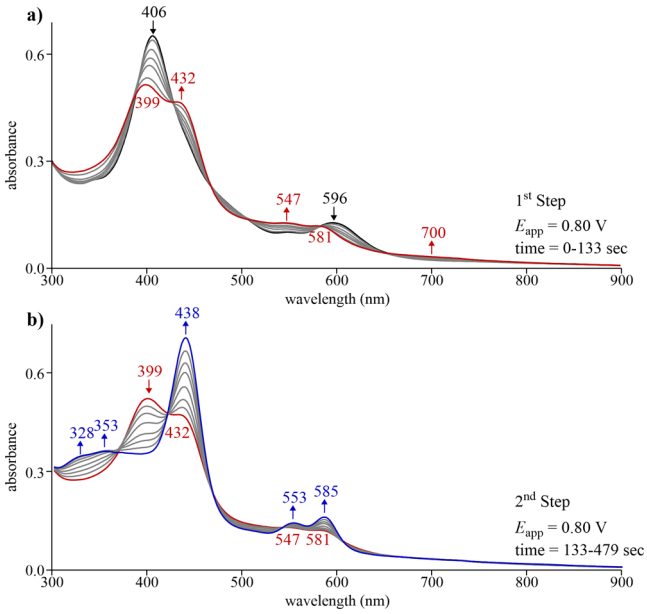

Figure 6. UV−vis spectral changes of $\{Re[TPC]\}_2$ associated with the first oxidation in CH_2Cl_2/0.1 M TBAP where (a) is the first step and (b) is the second step.

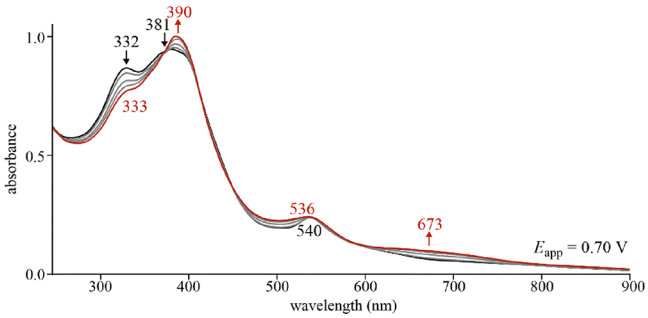

Figure 7. UV−vis spectral changes of $\{\{Ru[TpOMePC]\}_2$ upon the first oxidation in CH_2Cl_2/0.1 M TBAP. *Note*: This process is reversible on the thin layer time scale.

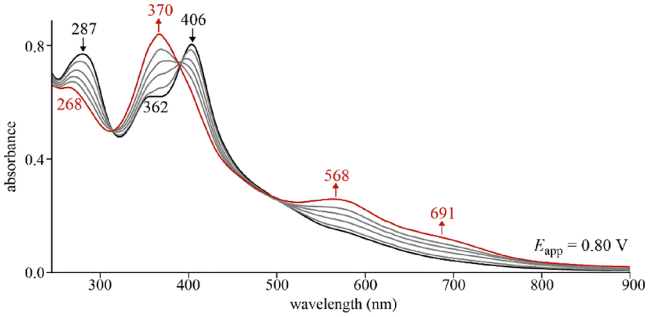

Figure 8. UV−vis spectral changes of $\{OsTpOMePC\}_2$ upon the first oxidations in CH_2Cl_2/0.1 M TBAP. *Note*: This process is reversible on the thin layer time scale, but the subsequent oxidation (not shown) was found to be irreversible.

the corrole, but oxidation does. In other words, while the reductions are likely to be metal-centered, the oxidations appear to be corrole-centered.

All-electron scalar-relativistic DFT calculations (OLYP[38,39]-D3[40]/STO-TZP) with full geometry optimizations were carried out on the neutral, anionic, and cationic states of

https://doi.org/10.1021/acsorginorgau.2c00030
ACS Org. Inorg. Au 2023, 3, 35−40

$\{M[TPC]\}_2$ (M = Re, Ru, Os) in vacuum and in the presence of a solvent (CH_2Cl_2 described via the COSMO[41] solvation model). Key quantitative results are depicted in Tables 2 and 3, while Figures 9 and 10 present spin density plots of the ionized states and the HOMO and LUMO of the neutral species, respectively. Consistent with electrochemical oxidation potentials, the calculations reveal very similar ionization potentials (IP) for the three compounds. Also, as expected, the HOMOs of the neutral species and the spin densities of the singly oxidized complexes are found to be predominantly localized on the corrole ligand. In contrast, the calculated electron affinities (EA) vary considerably among the three compounds following the order Re > Ru > Os, a trend that nicely mirrors the order of the reduction potentials (see Table 1 and Figures 1 and 2). Also, as expected on the basis of the spectroelectrochemistry results, the computed spin densities of the singly reduced Re and Ru compounds are exclusively localized on the metal atoms, reflecting the addition of an electron to a δ^* and π^* MO, respectively.

Table 2. Selected OLYP-D3/ZORA/STO-TZP Energetics (eV): Adiabatic Ionization Potential (IP_a), Electron Affinity (EA_a), and Singlet−Triplet Gap ($E_{S\text{-}T(a)}$) in the Gas Phase; Also, $E_{S\text{-}T(a)}$ and Kohn−Sham HOMO−LUMO Gap $\Delta\varepsilon$ in the Presence of a Solvent (COSMO/CH_2Cl_2)

compound	gas phase			COSMO/CH_2Cl_2	
	IP_a	EA_a	$E_{S\text{-}T(a)}$	$E_{S\text{-}T(a)}$	$\Delta\varepsilon$
$\{Re[TPC]\}_2$	5.41	2.62	0.14	0.13	0.15
$\{Ru[TPC]\}_2$	5.46	1.92	0.92	0.92	1.05
$\{Os[TPC]\}_2$	5.44	1.48	1.37	1.37	1.54

Table 3. Scalar-Relativistic OLYP/STO-TZP (COSMO) Mulliken Spin Populations Summed over the Bimetal Unit and All Ligand Atoms for the Anionic and Cationic States of the Compounds Studied

compound	anion		cation	
	M_2	ligand	M_2	ligand
$\{Re[TPC]\}_2$	1.019	−0.019	0.344	0.657
$\{Ru[TPC]\}_2$	0.756	0.244	0.165	0.837
$\{Os[TPC]\}_2$	0.081	0.919	0.111	0.889

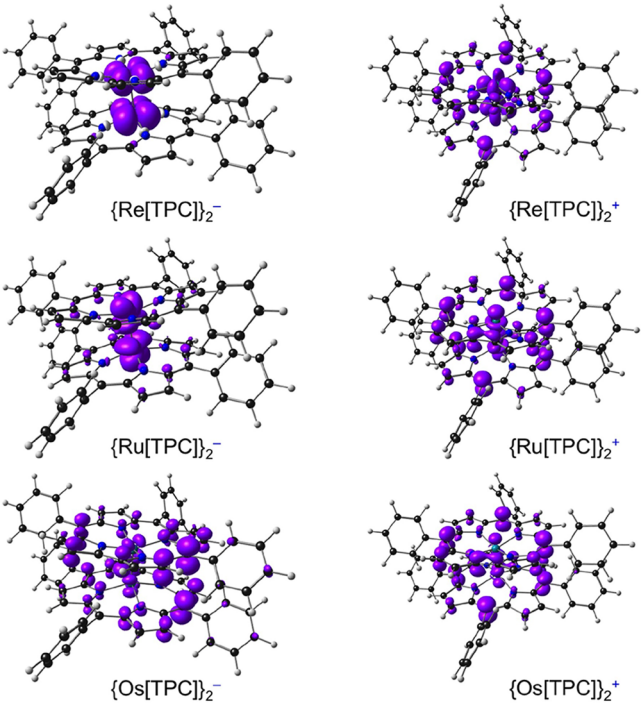

Figure 9. Scalar-relativistic OLYP/STO-TZP (COSMO) spin density profiles of $\{M[TPC]\}_2^{\pm}$ (M = Re, Ru, and Os) ions.

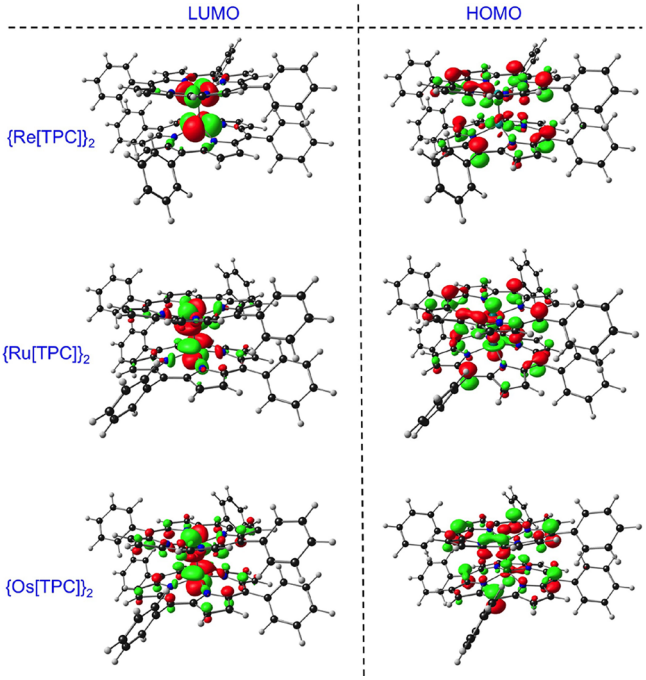

Figure 10. Scalar-relativistic OLYP/STO-TZP (COSMO) frontier MOs of neutral $\{M[TPC]\}_2$ (M = Re, Ru, and Os) complexes.

That said, the DFT results do present a few surprises, one being that the oxidations are not *exclusively* corrole-centered. The combined ligand spin populations in the cationic states (Table 3) add up to about 66, 85, and 90% for Re, Ru, and Os, respectively, meaning that the singly oxidized Os dimer has the most π-cation radical character, while that of the Re dimer has the least. This result seems consistent with spectroelectrochemical data, which shows that the first oxidation of the Re−Re corrole dimer proceeds via two-steps and can be interpreted as an initial electron abstraction from the corrole ligand followed by a rearrangement of the electron configuration via an intramolecular electron transfer from the Re−Re metal center to the electron *hole* in the macrocycle. Another interesting result involves the nature of reduction of the Os corrole dimer. Although the LUMO of neutral $\{Os[TPC]\}_2$ is qualitatively similar to that of neutral $\{Ru[TPC]\}_2$, with a bimetal π^* orbital at its core (Figure 10), most of the spin density on the singly reduced Os dimer leaks onto the corrole ligands, reflecting a much greater relativistic destabilization of the Os(5d) orbitals relative to Ru(4d) orbitals (Table 3).[21,42]

In summary, we have presented a first major, comparative UV−visible−NIR spectroelectrochemical study of metal−metal multiple-bonded metallocorrole complexes. The broad conclusion that oxidations of the metallocorrole dimers are largely corrole-centered, whereas the reductions are significantly mostly metal-centered, is largely confirmed by DFT

https://doi.org/10.1021/acsorginorgau.2c00030
ACS Org. Inorg. Au 2023, 3, 35−40

calculations. The calculations do, however, afford a more nuanced picture with respect to the spin densities of the ionized states. To what extent peripheral substituents might impact the partitioning of the spin densities of the ionized states between the bimetal unit and the corroles remains a question for future studies.

EXPERIMENTAL SECTION

Cyclic voltammograms (CVs) were obtained on an EG&G Model 263A potentiostat equipped with a three-electrode system: a glassy carbon working electrode, a platinum wire counter electrode, and a saturated calomel reference electrode (SCE). CH_2Cl_2 used as solvent was predried and distilled from P_2O_5. Tetrakis(*n*-butyl)ammonium perchlorate (TBAP) was used as the supporting electrolyte. The SCE was separated from the sample solution by a fritted-glass bridge of low porosity filled with CH_2Cl_2-TBAP solution. Before each electrochemical measurement, sample solutions were purged with argon for at least 5 min and an argon blanket was maintained over the solutions during measurements. Low temperature CV measurements were made by immersing the cell in an appropriate dry ice/acetone mixture.

Thin-layer UV−vis spectroelectrochemical experiments were performed with a home-built thin-layer cell equipped with a transparent platinum net working electrode. Potentials were applied and monitored with an EG&G PAR Model 173 potentiostat. Time-resolved UV−visible spectra were recorded with a Hewlett-Packard Model 8453 diode array spectrophotometer. High-purity N_2 from Trigas was used to deoxygenate the solution and kept over the solution during each experiment.

COMPUTATIONAL METHODS

All DFT calculations were carried out with the well-tested OLYP exchange-functional augmented with Grimme's D3 dispersion corrections as implemented in the ADF 2019 program system.[43] Relativistic effects were taken into account with the zeroth-order regular approximation (ZORA) applied as a scalar correction and specially optimized all-electron ZORA STO-TZP basis sets. For such calculations, a C_2 symmetry constraint was generally applied.

ASSOCIATED CONTENT

Supporting Information

The Supporting Information is available free of charge at https://pubs.acs.org/doi/10.1021/acsorginorgau.2c00030.

DFT optimized coordinates of the neutral, oxidized, and reduced $\{M[TPC]\}_2$ molecules (M = Ru, Os, and Re) (PDF)

AUTHOR INFORMATION

Corresponding Authors

Abhik Ghosh − *Department of Chemistry, UiT − The Arctic University of Norway, N-9037 Tromsø, Norway;* orcid.org/0000-0003-1161-6364; Email: abhik.ghosh@uit.no

Karl M. Kadish − *Department of Chemistry, University of Houston, Houston, Texas 77204-5003, United States;* orcid.org/0000-0003-4586-6732; Email: kkadish@uh.edu

Authors

W. Ryan Osterloh − *Department of Chemistry, University of Houston, Houston, Texas 77204-5003, United States;* orcid.org/0000-0001-9127-2519

Jeanet Conradie − *Department of Chemistry, UiT − The Arctic University of Norway, N-9037 Tromsø, Norway; Department of Chemistry, University of the Free State, Bloemfontein 9300, South Africa;* orcid.org/0000-0002-8120-6830

Abraham B. Alemayehu − *Department of Chemistry, UiT − The Arctic University of Norway, N-9037 Tromsø, Norway;* orcid.org/0000-0003-0166-8937

Complete contact information is available at: https://pubs.acs.org/10.1021/acsorginorgau.2c00030

Notes

The authors declare no competing financial interest.

ACKNOWLEDGMENTS

This work was supported by the Research Council of Norway (grant 324139 to A.G.), the Robert A. Welch Foundation (grant E-680 to K.M.K.), and National Research Foundation (NRF) of South Africa (grants 129270 and 132504).

REFERENCES

(1) Cotton, F. A.; Curtis, N. F.; Harris, C. B.; Johnson, B. F. G.; Lippard, S. J.; Mague, J. T.; Robinson, W. R.; Wood, J. S. Mononuclear and Polynuclear Chemistry of Rhenium (III): Its Pronounced Homophilicity. *Science* **1964**, *145*, 1305−1307.

(2) Cotton, F. A. Metal-Metal Bonding in $[Re_2X_8]^{2-}$ Ions and Other Metal Atom Clusters. *Inorg. Chem.* **1965**, *4*, 334−336.

(3) Cotton, F. A. Discovering and understanding multiple metal-to-metal bonds. *Acc. Chem. Res.* **1978**, *11*, 225−232.

(4) Trogler, W. C.; Gray, H. B. Electronic spectra and photochemistry of complexes containing quadruple metal-metal bonds. *Acc. Chem. Res.* **1978**, *11*, 232−239.

(5) Cotton, F. A.; Nocera, D. C. The Whole Story of the Two-Electron Bond, with the δ Bond as a Paradigm. *Acc. Chem. Res.* **2000**, *33*, 483−490.

(6) Cotton, F. A., Murillo, C. A., Walton, R. A. Eds., *Multiple bonds between metal atoms*; Springer: New York, 2005, 818, DOI: 10.1007/b136230

(7) Collman, J. P.; Arnold, H. J. Multiple Metal-Metal Bonds in 4d and 5d Metal-Porphyrin Dimers. *Acc. Chem. Res.* **1993**, *26*, 586−592.

(8) Collman, J. P.; Boulatov, R. Heterodinuclear Transition-Metal Complexes with Multiple Metal−Metal Bonds. *Angew. Chem., Int. Ed.* **2002**, *41*, 3927−4154.

(9) Alemayehu, A. B.; McCormick-McPherson, L. J.; Conradie, J.; Ghosh, A. Rhenium Corrole Dimers: Electrochemical Insights into the Nature of the Metal−Metal Quadruple Bond. *Inorg. Chem.* **2021**, *60*, 8315−8321.

(10) Collman, J. P.; Garner, J. M.; Hembre, R. T.; Ha, Y. Relative Strength of 4d vs 5d d-bonds: Rotational Barriers of Isostructural Molybdenum and Tungsten Porphyrin Dimers. *J. Am. Chem. Soc.* **1992**, *114*, 1292−1301.

(11) Collman, J. P.; Arnold, H. Delta bonds and rotational barriers in 4d and 5d metal-porphyrin dimers. *J. Cluster Sci.* **1994**, *5*, 37−66.

(12) Kim, J. C.; Goedken, V. L.; Lee, B. M. Synthesis and rotational barrier of tungsten(II) porphyrin dimer, $[W(TPP)]_2$ (TPP = Tetraphenylporphyrin). *Polyhedron* **1996**, *15*, 57−62.

(13) Conradie, J.; Vazquez-Lima, H.; Alemayehu, A. B.; Ghosh, A. Comparing Isoelectronic, Quadruple-Bonded Metalloporphyrin and Metallocorrole Dimers: Scalar-Relativistic DFT Calculations Predict a >1 eV Range for Ionization Potential and Electron Affinity. *ACS Phys. Chem Au* **2022**, *2*, 70−78.

(14) A potential explanation is that certain quadruple-bonded compounds are difficult to handle, on account of exceptionally low ionization potentials,[15,16] which might have precluded solution-phase measurements.

(15) Cotton, F. A.; Gruhn, N. E.; Gu, J.; Huang, P.; Lichtenberger, D. L.; Murillo, C. A.; Van Dorn, L. O.; Wilkinson, C. C. Closed-Shell

Molecules That Ionize More Readily Than Cesium. *Science* **2002**, *298*, 1971−1974.
(16) Cotton, F. A.; Donahue, J. P.; Lichtenberger, D. L.; Murillo, C. A.; Villagrán, D. Expeditious Access to the Most Easily Ionized Closed-Shell Molecule, $W_2(hpp)_4$. *J. Am. Chem. Soc.* **2005**, *127*, 10808−10809.
(17) Simkhovich, L.; Luobeznova, I.; Goldberg, I.; Gross, Z. Mono- and Binuclear Ruthenium Corroles: Synthesis, Spectroscopy, Electrochemistry, and Structural Characterization. *Chem. − Eur. J.* **2003**, *9*, 201−208.
(18) Kadish, K. M.; Burdet, F.; Jerome, F.; Barbe, J.-M.; Ou, Z.; Shao, J.; Guilard, R. Synthesis, Physicochemical and Electrochemical Properties of Metal-Metal Bonded Ruthenium Corrole Homodimers. *J. Organomet. Chem.* **2002**, *652*, 69−76.
(19) Van Caemelbecke, E.; Phan, T.; Osterloh, W. R.; Kadish, K. M. Electrochemistry of metal-metal bonded diruthenium complexes. *Coord. Chem. Rev.* **2021**, *434*, 213706.
(20) Alemayehu, A. B.; Vazquez-Lima, H.; Gagnon, K. J.; Ghosh, A. Stepwise Deoxygenation of Nitrite as a Route to Two Families of Ruthenium Corroles: Group 8 Periodic Trends and Relativistic Effects. *Inorg. Chem.* **2017**, *56*, 5285−5294.
(21) Alemayehu, A.; McCormick, L. J.; Vazquez-Lima, H.; Ghosh, A. Relativistic Effects on a Metal−Metal Bond: Osmium Corrole Dimers. *Inorg. Chem.* **2019**, *58*, 2798−2806.
(22) Fang, Y.; Ou, Z.; Kadish, K. M. Electrochemistry of Corroles in Nonaqueous Media. *Chem. Rev.* **2017**, *117*, 3377−3419.
(23) The oxidation potentials are similar to those found for corrole derivatives of other +III cations, such as Co(III),[24,25,26] Ga(III),[27] Rh(III),[24,28] Ir(III),[29,30] and Au(III).[31,32]
(24) Ganguly, S.; Renz, D.; Giles, L. J.; Gagnon, K. J.; McCormick, L. J.; Conradie, J.; Sarangi, R.; Ghosh, A. Cobalt- and Rhodium-Corrole-Triphenylphosphine Complexes Revisited: the Question of a Noninnocent Corrole. *Inorg. Chem.* **2017**, *56*, 14788−14800.
(25) Ganguly, S.; Conradie, J.; Bendix, J.; Gagnon, K. J.; McCormick, L. J.; Ghosh, A. Electronic Structure of Cobalt−Corrole−Pyridine Complexes: Noninnocent Five-Coordinate Co(II) Corrole−Radical States. *J. Phys. Chem. A* **2017**, *121*, 9589−9598.
(26) Li, B.; Ou, Z.; Meng, D.; Tang, J.; Fang, Y.; Liu, R.; Kadish, K. Cobalt Triarylcorroles Containing One, Two or Three Nitro Groups. Effect of NO_2 Substitution on Electrochemical Properties and Catalytic Activity for Reduction of Molecular Oxygen in Acid Media. *J. Inorg. Biochem.* **2014**, *136*, 130−139.
(27) Bendix, J.; Dmochowski, I. J.; Gray, H. B.; Mahammed, A.; Simkhovich, L.; Gross, Z. Structural, Electrochemical, and Photophysical Properties of Gallium(III) 5,10,15-Tris(pentafluorophenyl)-corrole. *Angew. Chem., Int. Ed.* **2000**, *39*, 4048−4051.
(28) Simkhovich, L.; Mahammed, A.; Goldberg, I.; Gross, Z. Synthesis and Characterization of Germanium, Tin, Phosphorus, Iron, and Rhodium Complexes of Tris(Pentafluorophenyl)Corrole, and the Utilization of the Iron and Rhodium Corroles as Cyclopropanation Catalysts. *Chem. − Eur. J.* **2001**, *7*, 1041−1055.
(29) Palmer, J. H.; Durrell, A. C.; Gross, Z.; Winkler, J. R.; Gray, H. B. Iridium Corroles. *J. Am. Chem. Soc.* **2008**, *130*, 7786−7787.
(30) Thomassen, I. K.; McCormick-McPherson, L. J.; Borisov, S. M.; Ghosh, A. Iridium Corroles Exhibit Weak Near-Infrared Phosphorescence but Efficiently Sensitize Singlet Oxygen Formation. *Sci. Rep.* **2020**, *10*, 7551.
(31) Thomas, K. E.; Alemayehu, A. B.; Conradie, J.; Beavers, C.; Ghosh, A. Synthesis and Molecular Structure of Gold Triarylcorroles. *Inorg. Chem.* **2011**, *50*, 12844−12851.
(32) Thomas, K. E.; Vazquez-Lima, H.; Fang, Y.; Song, Y.; Gagnon, K. J.; Beavers, C. M.; Kadish, K. M.; Ghosh, A. Ligand Noninnocence in Coinage Metal Corroles: A Silver Knife-Edge. *Chem. − Eur. J.* **2015**, *21*, 16839−16847.
(33) The oxidation potentials are 300−500 mV lower than those of corrole derivatives of high oxidation state metal ions such as 99Tc(V),[34] Re(V),[35,36] Ru(VI),[37]and Os(VI).[38]
(34) Einrem, R. F.; Braband, H.; Fox, T.; Vazquez-Lima, H.; Alberto, R.; Ghosh, A. Synthesis and molecular structure of ^{99}Tc Corroles. *Chem. − Eur. J.* **2016**, *22*, 18747−18751.
(35) Einrem, R. F.; Gagnon, K. J.; Alemayehu, A. B.; Ghosh, A. Metal-Ligand Misfits: Facile Access to Rhenium-Oxo Corroles by Oxidative Metalation. *Chem. − Eur. J.* **2016**, *22*, 517−520.
(36) Alemayehu, A. B.; Teat, S. J.; Borisov, S. M.; Ghosh, A. Rhenium-Imido Corroles. *Inorg. Chem.* **2020**, *59*, 6382−6389.
(37) Alemayehu, A. B.; Gagnon, K. J.; Terner, J.; Ghosh, A. Oxidative Metalation as a Route to Size-Mismatched Macrocyclic Complexes: Osmium Corroles. *Angew. Chem., Int. Ed.* **2014**, *53*, 14411−14414.
(38) Handy, N. C.; Cohen, A. J. Left-right correlation energy. *Mol. Phys.* **2001**, *99*, 403−412.
(39) Lee, C.; Yang, W.; Parr, R. G. Development of the Colle-Salvetti correlation-energy formula into a functional of the electron density. *Phys. Rev. B* **1988**, *37*, 785−789.
(40) Grimme, S.; Anthony, J.; Ehrlich, S.; Krieg, H. A Consistent and Accurate *Ab Initio* Parametrization of Density Functional Dispersion Correction (DFT-D) for the 94 Elements H-Pu. *J. Chem. Phys* **2010**, *132*, 154104.
(41) Klamt, A.; Schüürmann, G. COSMO: A New Approach to Dielectric Screening in Solvents with Explicit Expressions for the Screening Energy and Its Gradient. *J. Chem. Soc., Perkin Trans* **1993**, *2*, 799−805.
(42) Pyykkö, P. Relativistic Effects in Chemistry: More Common Than You Thought. *Annu. Rev. Phys. Chem.* **2012**, *63*, 45−64.
(43) Velde, G. T.; Bickelhaupt, F. M.; Baerends, E. J.; Guerra, C. F.; van Gisbergen, S. J. A.; Snijders, J. G.; Ziegler, T. Chemistry with ADF. *J. Comput. Chem.* **2001**, *22*, 931−967.

https://doi.org/10.1021/acsorginorgau.2c00030
ACS Org. Inorg. Au 2023, 3, 35−40